INSTITUTE OF PHYSICS PUBLISHING SMART MATERIALS AND STRUCTURES
Smart Mater. Struct. **12** (2003) 80–87 PII: S0964-1726(03)56116-X

Semi-active control of structures incorporated with magnetorheological dampers using neural networks

Zhao-Dong Xu[1,2,3], **Ya-Peng Shen**[1] **and Ying-Qing Guo**[2]

[1] Institute of Architecture and Mechanics, Xi'an Jiaotong University, Xi'an, China
[2] Institute of Civil Engineering, Southeast University, Nanjing, China

E-mail: xuzhd@mail.xjtu.edu.cn

Received 17 December 2001, in final form 23 September 2002
Published 10 January 2003
Online at stacks.iop.org/SMS/12/80

Abstract
Semi-active control of buildings and structures with magnetorheological (MR) dampers for earthquake hazard mitigation represents a relatively new research area. In this paper, the Bingham model of MR damper is introduced, and the formula relating the yielding shear stress and the control current of MR dampers is put forward that matches the experimental data. Then an on-line real-time control method for semi-active control of structures with MR dampers is proposed. This method considers the time-delay problem of semi-active control, which can solve distortion of the responses of structures. Finally, through a numerical example of a three-storey reinforced concrete structure, a comparison is made between controlled structure and uncontrolled structure. The calculated results show that MR dampers can reduce the seismic responses of structures effectively. Moreover, the on-line real-time control method is compared with the traditional elastoplastic time-history analysis method, and the efficacy of the on-line real-time control method is demonstrated. In addition, the Levenberg–Marquardt algorithm is used to train the on-line control neural network, and studies show that the algorithm has a very fast convergence rate.

1. Introduction

Seismic design of structures is an important and tough job. The traditional approach to seismic hazard mitigation is to design structures with sufficient strength capacity and the ability to deform in a ductile manner. Recently, newer concepts of structural control, including both passive and active control systems, have been growing in acceptance and may preclude the necessity of allowing for inelastic deformations in the structural system. Passive control devices, such as viscoelastic damper, viscous fluid damper, friction damper and metallic damper can partially absorb structural vibration energy and reduce seismic responses of structures [1]. These passive devices are relatively simple and easily implemented. However, the effectiveness of passive control is limited due to the passive nature of devices and the random nature of earthquake events. Active control devices, including active mass damper and active tendon system, can be more effective in reducing the seismic structural responses than passive control devices because feedback or feedforward control systems are used [2]. However, the complicated control system and the large power requirement during a strong earthquake hamper their implementation in practice. Therefore, a compromise between passive and active control systems has been developed recently in the form of semi-active control systems. Semi-active control systems maintain the reliability of passive control systems while taking advantage of the adjustable parameter characteristics of an active control system [3]. Among semi-active control devices, the magnetorheological (MR) damper is typical of a smart damper.

Note that in active control or semi-active control, sampling of the sensor data, transmission and calculation of signal and

[3] Author to whom any correspondence should be addressed.

infliction of control force are time consuming procedures. Moreover, control force is based on feedback from sensors that measure the excitation and/or the responses of the structure [4]. Although the sensor data can be sampled at a very fast rate, the control system must complete its computation and send out the control signal to the damper before it can use the next sample of the sensor data. Therefore, in closed-loop structural control systems the output rate dictates the effective sampling period, which, in most cases, is much slower than the input sampling rate [5]. Since the control forces are calculated according to the last responses of structures in the traditional time-history analysis method, an inherent time-delay problem lies in the traditional method. For the building structure, too small a sampling time will lead to tremendous calculation, especially in the elastoplastic analysis of structures. Generally, the sampling time is chosen in the range of 0.001–0.1 s, which is a larger time delay. Some studies have already shown the importance of solving the time-delay problem in control systems [5–8]. If time delay is not properly dealt with, it may have adverse effects on the control actions. For instance, it may cause structures to become unstable and more dangerous [5, 8]. Therefore an effective way to solve this problem is to find an appropriate method, which can predict the future responses of structures according to the responses and the acceleration excitation inputs of previous epochs.

The neural network technique can be used for this purpose. The main advantage of the neural network approach is that identification of an unknown system and evaluation of responses can be performed without building a mathematical model of the system [8]. Many investigators have investigated the use of a neural network technique for active and semi-active control of structures, and significant progress has been made. A backpropagation-through-time neural controller (BTTNC) for active control of structure was developed by Chen *et al* [9]. A new neural-network-based control algorithm has been developed and tested in the computer simulation of active control of a three-storey frame structure by Ghaboussi *et al* [10]. A conventional feedforward controller and a neurocontroller were designed to compensate for the adverse effects of actuator dynamics and computational phase delay by Nikzad *et al* [5]. Implementation of a neural network for system identification and vibration suppression of a smart structure was conducted by Yang [11]. An experimental study of identification and control of structures using neural networks was carried out by Bani-Hani *et al* [12]. Recently, a neuron-control method was proposed for semi-active vibration control of stay cables using MR dampers by Ni *et al* [13].

In this paper, the common mathematical model of MR dampers (the Bingham model) is introduced, and a formula relating the yielding shear stress and the control current of MR dampers is put forward in agreement with the experimental data. The equations of motion of a multi-storey frame structure with smart damper brace systems are then established. The on-line real-time control strategy of the smart structure with MR dampers is proposed. A four-layer feedforward neural network, trained on-line under the Levenberg–Marquardt (LM) algorithm, is used to predict the future responses of the smart structure. In order that the responses of the smart structure satisfy the seismic requirements of the structure or are reduced most effectively, the control current applied to the MR dampers is calculated according to the predicting responses of the structure. Finally, through a numerical simulation of a three-story reinforced concrete frame structure with MR dampers and without MR dampers by the on-line real-time control method and the traditional elastoplastic time-history analysis method, it is found that MR dampers can reduce the seismic responses of the structure effectively and the on-line real-time control method is more accurate than the traditional elastoplastic time-history analysis method in controlling the smart structure due to its solution to time delay.

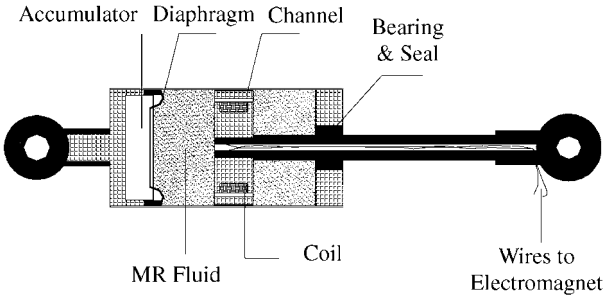

Figure 1. Schematic illustration of MR damper.

2. Governing equations

2.1. Modeling of MR dampers

MR dampers typically consist of a hydraulic cylinder containing micrometer-sized magnetically polarizable particles dispersed in hydrocarbon oil, as shown in figure 1. In the presence of a strong magnetic field, the particles polarize and offer an increased resistance to flow. By varying the magnetic field, the mechanical behavior of MR dampers can be modulated. Since MR fluid can be changed from a viscous fluid to a yielding solid within milliseconds and the resulting damping force can be considerably large with a low-power requirement, MR dampers are applicable to large civil engineering structures [14].

Many investigators, such as Spencer *et al* [15], Carlson and Spencer [16], Dyke *et al* [17] and Wereley *et al* [18], have studied the mechanical properties of MR dampers. The most popular model of MR damper is the Bingham model [19, 20], in which MR dampers are assumed to have a friction component augmented by a Newtonian viscosity component as shown in figure 2, and the relationship between stress and strain can be expressed as follows:

$$\tau = \eta\dot{\gamma} + \tau_y \operatorname{sgn}(\dot{\gamma}) \tag{1}$$

where τ is the shear stress in fluid, η is the Newtonian viscosity, independent of the applied magnetic field, $\dot{\gamma}$ is the shear strain rate and τ_y is the yielding shear stress controlled by the applied field. Phillips *et al* [21] derived the force–displacement relationship of MR dampers in terms of equation (1) as

$$F = \frac{12\eta L A_p^2}{\pi D h_d^3}\dot{u}(t) + \frac{3L\tau_y}{h_d}A_p \operatorname{sgn}[\dot{u}(t)] \tag{2}$$

where L is the length of the piston, A_p is the cross-sectional area of the piston, D is the inner diameter of the vat, h_d is the

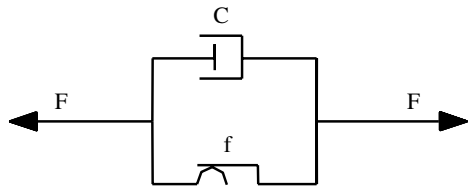

Figure 2. Bingham model.

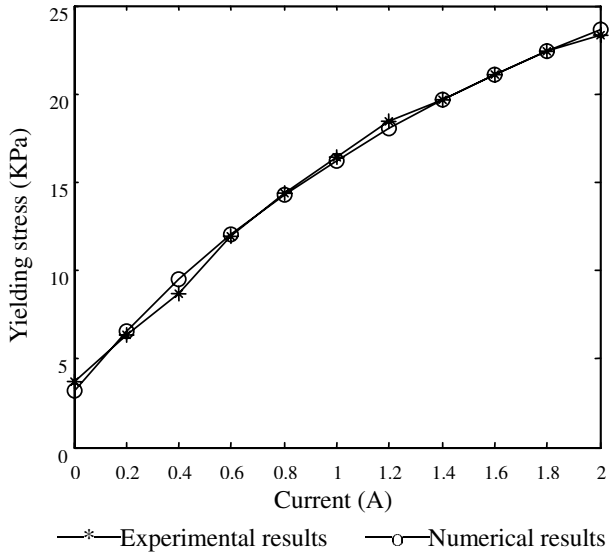

Figure 3. Comparison between the experimental and numerical results.

diameter of the small orifice in the piston and $u(t)$ is the relative displacement of the piston to the vat. The yielding shear stress τ_y is the function of the applied field, which means τ_y is the function of the controlled current I. The experiment on MR dampers is that of Professor Ou [22], the MR damper fluid was developed by Fudan University in China, and the viscosity η is 0.9 Pa m. For the dampers, the effective length of the piston L is 40 mm, the gap h is 2 mm and the inner diameter of the vat is 80 mm. We find that the relationship between the yielding shear stress τ_y and the control current I obeys the index function law. In accordance with the experimental data, the yielding shear stress τ_y is related to the control current I by

$$\tau_y = A_1 \mathrm{e}^{-I} + A_2 \ln(I + \mathrm{e}) + A_3 I \tag{3}$$

where the coefficients A_1, A_2 and A_3 depend on the property of the MR fluid in the MR damper. For the MR fluid in this test, $A_1 = -11\,374$, $A_2 = 14\,580$, $A_3 = 1281$, and e is the natural constant. A comparison between the experimental results and the numerical prediction by equation (3) on the current-dependent yield stress is shown in figure 3. It can be seen that the numerical results agree well with the experimental results.

2.2. Equations of motion of controlled structure

For frame structures, MR dampers are usually placed on chevron braces as shown in figure 4. In terms of stiffness, the smart damper–chevron brace system can be treated as a damper and a spring connected in series. For MR dampers to

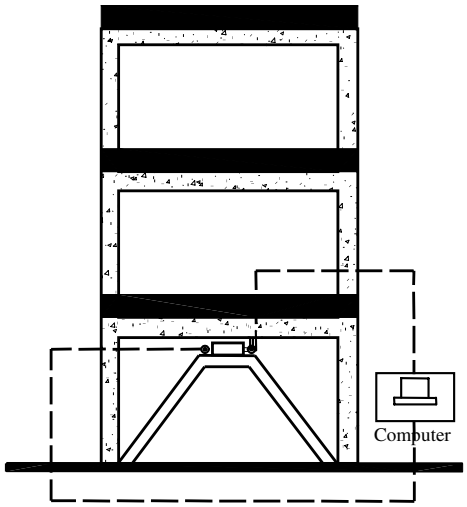

Figure 4. Schematic illustration of smart structure.

function properly, the stiffness of the chevron braces is usually strong. Accordingly, the stiffness of chevron braces can be neglected to simplify calculation, and the equations of motion of the structure with MR dampers can be written as

$$\boldsymbol{M}\ddot{\boldsymbol{x}} + \boldsymbol{C}\dot{\boldsymbol{x}} + \boldsymbol{K}\boldsymbol{x} = -\boldsymbol{M}\Gamma\ddot{x}_g - \boldsymbol{B}\boldsymbol{f}_d \tag{4}$$

where $\boldsymbol{M}, \boldsymbol{C}$ and $\boldsymbol{K}$ are the mass, damping and stiffness matrices of the structure respectively, $\boldsymbol{x}$ is the vector of the relative displacements of the floors of the structure, Γ is the column vector of ones, $\ddot{x}_g$ is the earthquake acceleration excitation, $\boldsymbol{B}$ is the matrix determined by the placement of MR dampers in the structure, $\boldsymbol{f}_d = [f_{d1}, f_{d2}, \ldots, f_{dn}]^{\mathrm{T}}$ is the vector of control forces produced by MR dampers, and f_{dn} is the control force of the nth floor.

The seismic responses of the structure with MR dampers expressed as equation (4) can be calculated by the time-history analysis method [23]. But in this method, the control forces are calculated according to the seismic responses of structures in the previous epochs. As a result, the control forces may be distorted due to time delay. Such distortion usually has adverse effects on the control actions. Furthermore, semi-active control has inherent time delay. Therefore, an effective way to solve this problem is to find an appropriate method which can predict future responses of the structure and control the structure on-line. The neural network technique has some advantages, such as identification and prediction, and it is considered to be the best method to solve the time-delay problem [5, 6, 24].

3. Semi-active control using neural networks

3.1. The traditional control method

The traditional analysis method used in the controlled structure is the time-history analysis method. For the reinforced concrete structure, the trilinear stiffness degeneration model [25] is adopted to simulate the structure. The relationship curve between the stiffness and inter-storey drift of each floor is illustrated in figure 5. For the structure with MR dampers, the control current I is initially set as zero. The dynamic responses of structures are then calculated. If the inter-storey

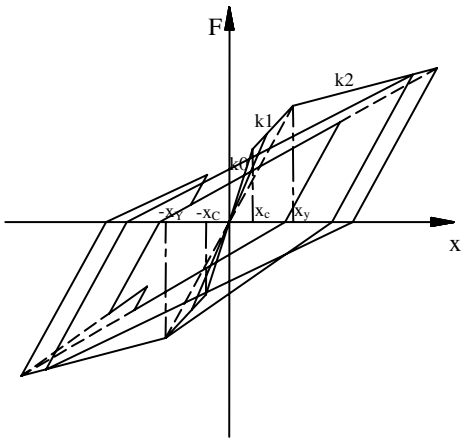

Figure 5. The trilinear stiffness degeneration model.

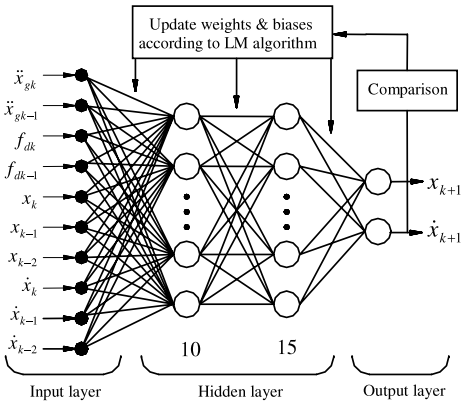

Figure 6. The neural network architecture.

drift of some a floor is not less than $h/450$, where h is the storey height, the control current of the MR dampers in this floor should be increased by an amount ΔI. The dynamic responses of structures are re-calculated for the new control current. Such a computation is repeated until the inter-storey drift of the floor satisfies the objective request or the control current reaches the maximum value $I_{\max}$. When the control current is determined, the dynamic responses of structures can be calculated, and the stiffness of each floor can be evaluated according to the responses of structures. Then the next epoch calculation can begin.

For the elastoplastic time-history analysis method, the control forces produced by MR dampers is based on the previous responses of structures instead of the current responses of structures. As a result, an inherent time-delay problem exists in this method. In order to solve this problem, the neural network technique is adopted to predict the responses of structures. The control forces are calculated according to the predicted responses.

3.2. Neural networks based on the LM algorithm

Neural networks are simplified models of the biological structure found in human brains. These models consist of elementary processing units (also called neurons). It is the large amount of interconnections between these neurons and their capability to learn from data, that makes neural networks a strong predicting and classification tool. In this study, the neural network approach is selected to predict the seismic responses of structures with MR dampers. Many neural networks are currently available, which can be divided into two main types: feedforward neural networks and feedback neural networks.

In this paper, a four-layer feedforward neural network is adopted, which consists of an input layer, two hidden layers and an output layer (as shown in figure 6). The inputs to the neural network are the delayed earthquake accelerations, the delayed control forces and the delayed seismic responses.

The net input net_k of neuron k in some layer and the output O_k of the same neuron are calculated by

$$\text{net}_k = \sum w_{jk} O_j \tag{5}$$

$$O_k = f(\text{net}_k + \theta_k) \tag{6}$$

where w_{jk} is the weight between the jth neuron in the previous layer and the kth neuron in the current layer, O_j is the output of the jth neuron in the previous layer, $f(\cdot)$ is the neuron's activation function which can be a linear function, radial basis function or a sigmoid function, and θ_k is the bias of the kth neuron. If the bias θ_k is regarded as the additional input whose weight and input are θ_k and 1 respectively, the adjustment for the bias θ_k can be considered as the adjustment of a weight. In the following, the adjustment for biases is the same as the adjustment for weights.

In the neural network architecture as shown in figure 6, the logarithmic sigmoid transfer function is chosen as the activation function of the first hidden layer:

$$O_k = f(\text{net}_k + \theta_k) = \frac{1}{1 + \text{e}^{-(\text{net}_k + \theta_k)}}. \tag{7}$$

The tangent sigmoid transfer function is chosen as the activation function of the second hidden layer:

$$O_k = f(\text{net}_k + \theta_k) = \frac{1 - \text{e}^{-2(\text{net}_k + \theta_k)}}{1 + \text{e}^{-2(\text{net}_k + \theta_k)}}. \tag{8}$$

The linear transfer function is chosen as the activation function of the output layer:

$$O_k = f(\text{net}_k + \theta_k) = \text{net}_k + \theta_k. \tag{9}$$

We note that neural networks need be trained before predicting seismic responses. As the inputs are applied to the neural network, the network outputs $\hat{\boldsymbol{y}}$ are compared with the targets $\boldsymbol{y}$. The difference or error between both is processed back through the network to update the weights and biases of the neural network so that the network outputs more closely match the targets. The input and output data are usually represented by vectors called training pairs. The process as mentioned above is repeated for all the training pairs in the data set, until the network error converges to a threshold minimum defined by a corresponding performance function. In this paper, the mean square error (MSE) function is adopted.

For the training pairs p ($p = 1, 2, \ldots, P$), the performance function of the total system is defined as

$$E = \frac{1}{2}\sum_{p=1}^{P}\sum_{q=1}^{Q}[y_p(q) - \hat{y}_p(q)]^2 = \frac{1}{2}\sum_{p=1}^{P}\sum_{q=1}^{Q} e_q^2 \qquad (10)$$

where Q is the number of neurons in the output layer, e_q is the error of the qth neuron in the output layer.

In order to make the network outputs $\hat{\boldsymbol{y}}$ approach the targets $\boldsymbol{y}$, the weights are moved in the opposite direction of the gradient of the performance function [24]. The most popular algorithm used for training neural networks is the so-called backpropagation (BP) algorithm. The BP method is a gradient-descent-based optimization technique. The BP algorithm can be described by

$$\boldsymbol{w}^{i+1} = \boldsymbol{w}^i - \eta_0 \frac{\partial E}{\partial \boldsymbol{w}^i} \qquad (11)$$

where i is the iteration index, $\partial E/\partial \boldsymbol{w}^i$ is the gradient descent of criterion E with respect to the parameter matrix $\boldsymbol{w}^i$, and $\eta_0 > 0$ is the learning rate.

The BP algorithm has a simple structure and can be easily understood and implemented. However, the algorithm usually suffers from the drawback of slow convergence. This is due to the fact that the gradient-based approach has a first-order convergence characteristic. On the other hand, it has been investigated that the BP algorithm can be considered as a pure integral control procedure. This can be used to explain why the choice of the learning rate η_0 may often result in some contradiction [26], i.e. a large η_0 can obtain fast learning but also easily cause oscillation and instability, while a small η_0 can obtain stable learning but the learning process will be very slow.

A useful way to improve the BP algorithm is by using second-order convergence-based approaches such as the Gauss–Newton method or the LM method [24]. The LM method can be written as

$$\boldsymbol{w}^{i+1} = \boldsymbol{w}^i - \left[\frac{\partial^2 E}{\partial \boldsymbol{w}^{i^2}} + \mu \boldsymbol{I}\right]^{-1} \frac{\partial E}{\partial \boldsymbol{w}^i} \qquad (12)$$

where $\mu \geqslant 0$ is the learning factor and $\boldsymbol{I}$ is the unity matrix. If the Taylor series expansion is applied to error vector $\boldsymbol{e}$ ($\boldsymbol{e} = [e_1, e_2, \ldots, e_Q]^{\mathrm{T}}$) around the operating point, the first derivatives result in the Jacobian given by

$$\boldsymbol{J}^i = \begin{bmatrix} \frac{\partial e_1}{\partial w_1^i} & \frac{\partial e_1}{\partial w_2^i} & \cdots & \frac{\partial e_1}{\partial w_B^i} \\ \frac{\partial e_2}{\partial w_1^i} & \frac{\partial e_2}{\partial w_2^i} & \cdots & \frac{\partial e_2}{\partial w_B^i} \\ \vdots & \vdots & \ddots & \vdots \\ \frac{\partial e_Q}{\partial w_1^i} & \frac{\partial e_Q}{\partial w_2^i} & \cdots & \frac{\partial e_Q}{\partial w_B^i} \end{bmatrix}_{Q \times B} \qquad (13)$$

where Q is the number of neurons in the output layer and B is the number of weights. A series of changes are made for equation (12) [27], and the following equation can be obtained:

$$\boldsymbol{w}^{i+1} = \boldsymbol{w}^i - (\boldsymbol{J}^{i^T}\boldsymbol{J}^i + \mu \boldsymbol{I})^{-1}\boldsymbol{J}^{i^T}\boldsymbol{e}. \qquad (14)$$

Equation (14) is the calculating formula of the LM method. The basic steps of this method are as follows:

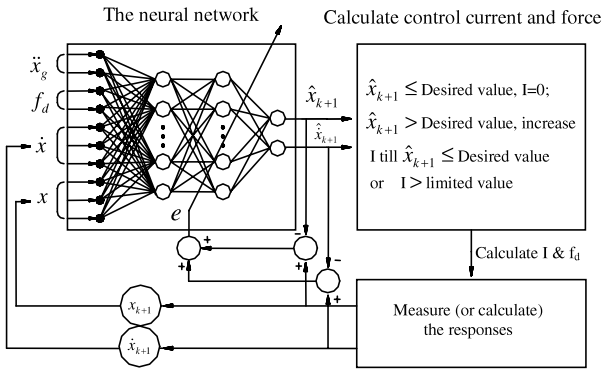

Figure 7. Structure of the proposed neural network controller.

(1) Set the initial weights (or bias) $\boldsymbol{w}^i = \boldsymbol{w}^0$, and take a large starting value of μ;
(2) Calculate the performance function $E(\boldsymbol{w}^i)$ and the Jacobian matrix $\boldsymbol{J}^i$;
(3) Calculate according to $\boldsymbol{w}^{i+1}$ equation (14);
(4) Is $|E(\boldsymbol{w}^{i+1})| \leqslant |E(\boldsymbol{w}^i)|$? If yes, decrease, i.e. $\mu^{i+1} = \alpha\mu^i (0 < \alpha < 1)$, where α is the decrease coefficient;
If no, increase μ by multiplying the increase coefficient β, i.e. $\mu^{i+1} = \beta\mu^i$ ($\beta > 1$).
(5) If the performance index E is less than target or the number of training epochs reaches the fixed number, then stop, else go to (2).

3.3. On-line real-time learning and control

The proposed on-line real-time learning and control architecture is shown in figure 7. The architecture consists of three parts to perform different tasks. The first part is the neural network to be trained on-line. When the number of the sample data pairs is less than 100, the training data pairs increase step-by-step during the earthquake. When the number of the sample data pairs is more than 100, the oldest data pair is abandoned in every training step, so that the number of the training data pairs remains 100. The neural network is trained to generate the one-step-ahead prediction of displacement $\hat{x}_{k+1}$ and velocity $\hat{\dot{x}}_{k+1}$. Inputs to this network are the delayed outputs $(x_{k-2}, x_{k-1}, x_k, \dot{x}_{k-2}, \dot{x}_{k-1}, \dot{x}_k)$, the delayed control forces (f_{dk-1}, f_{dk}) and the delayed earthquake inputs $(\ddot{x}_{g_{k-2}}, \ddot{x}_{g_{k-1}}, \ddot{x}_{g_k})$. The second part is to calculate control currents and control forces. If $\hat{x}_{k+1} \leqslant$ desired value (in this paper, $(\Delta_{k+1})_{\max} \leqslant h/450$ is adopted for the frame structure, where $(\Delta_{k+1})_{\max}$ is the maximum inter-storey drift and h is the storey height of the maximum inter-storey drift floor), set the control current of MR dampers $I = 0$; if $\hat{x}_{k+1} >$ desired value, increase the control current I (the current increment $\Delta I = 0.2$ A) and calculate the seismic responses of structures with MR dampers until $\hat{x}_{k+1}$ is less than or equal to the desired value or the control current I reaches the limited value (2 A for this paper). Then the control forces can be calculated by equations (2) and (3), and the responses of structures with MR dampers can be obtained by the elastoplastic time-history analysis method after the control current I is changed. The third part is to measure the actual responses of structures with MR dampers. In this paper, the calculated results by

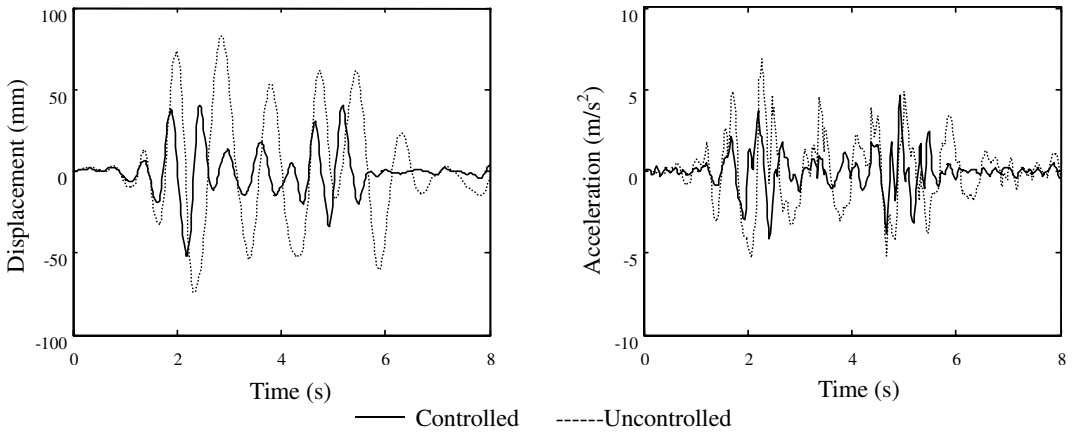

Figure 8. Response comparison of controlled and uncontrolled structure.

the elastoplastic time-history analysis method are used to substitute for the actual measured responses. The errors between the predicted responses and the actual responses are used to update the weights on-line.

4. Numerical example

To evaluate the on-line real-time method for the structure with MR dampers, a numerical example is considered in which a model of a three-storey reinforced concrete structure is controlled with one MR damper in the first floor, as shown in figure 4. In the elastoplastic analysis of the structure with MR dampers, the frame structure is simulated by the trilinear stiffness degeneration model as shown in figure 5 [25]. The stiffness of each floor changes in the fold line path as shown in figure 5 during the earthquake.

The model structure parameters are the mass vector $\boldsymbol{m} = [3.24\ 3.06\ 2.88] \times 10^4$ kg, the initial stiffness vector $\boldsymbol{k} = [1.86\ 2.60\ 2.60] \times 10^7$ N m^{-1}, the story height $\boldsymbol{h} = [4\ 3.3\ 3.3]$ m, the inter-story cracking drifts $\boldsymbol{\Delta}_c = [6.3\ 4.9\ 4.2]$ mm, the inter-story yielding drifts $\boldsymbol{\Delta}_y = [21.8\ 18.9\ 17.2]$ mm. The common MR damper as shown in figure 1 is adopted in this study. The MR fluid tested by Ou [22] is used in the MR damper, so the coefficients in equation (3) are $A_1 = -11\,374$, $A_2 = 14\,580$ and $A_3 = 1281$, and the viscosity η is 0.9 Pa m. The effective length of the piston L is 400 mm, the gap h_d is 2 mm, and the inner diameter of the vat is 100 mm.

In this example, the model of the structure is subjected to the north–south component of the 1940 El Centro earthquake with 400 gal acceleration amplitude, and the sampling time is 0.02 s, i.e. the delay time. We developed a Matlab program for the on-line real-time neural network control and elastoplastic analysis of the structure with MR dampers.

The top-floor displacement and acceleration responses of the structure with the MR damper by the on-line control method are compared with those of the structure without the MR damper, as shown in figure 8. Both the displacement and the acceleration responses of the controlled structure with the MR damper are reduced effectively. The maximum displacement of the uncontrolled structure is 82.91 mm, while the maximum displacement of the controlled structure is 51.47 mm. The displacement response is reduced by 37.92%. The maximum acceleration of the uncontrolled structure is 6.86 m s^{-2}, while the maximum acceleration of the controlled structure is 4.65 m s^{-2}. The acceleration response is reduced by 32.22%. It can also be shown that the displacement responses are reduced more effectively than the acceleration responses. This is due to the fact that control forces produced by MR dampers are equivalent to increasing stiffness and damping of structures: both are beneficial to decreasing displacement responses, while increasing of stiffness will possibly increase acceleration responses.

The responses of the structure with the MR damper are calculated by the traditional elastoplastic time-history analysis method and the on-line real-time control method. Figure 9 compares the displacement responses and the acceleration responses of the top floor for the on-line control method and the traditional method. The displacement and acceleration responses calculated by the on-line control method are smaller than those calculated by the traditional method, especially during the periods of 1.5–3 and 4.2–6.5 s. Recall that the traditional method does not consider the problem of time delay, which leads to distortion of the control forces and destabilization of the whole closed-loop control structure. This explains why the traditional method predicts increased oscillation compared to the on-line control method.

Figure 10 compares maximum displacement and maximum acceleration for the uncontrolled structure, the traditional controlled structure and the on-line controlled structure. Both the displacement and the acceleration responses are reduced effectively when MR dampers are used. At the same time, it can be clearly seen that the on-line control method can reduce the dynamic responses of the structure more effectively than the traditional control method, especially for the acceleration responses. Because the on-line control method disposes of the time-delay problem, the control forces produced by MR dampers are more accurate. Increasing the control forces blindly is equal to increasing the stiffness and the damping of the structure blindly, which will lead to increase of the dynamic responses, especially for acceleration responses.

The control current–time curves calculated by the on-line control method and the traditional time-history analysis method are plotted in figures 11(a) and (b), respectively. The control current of the MR damper varies in the range in 0–2 A when the earthquake excitation is strong during the

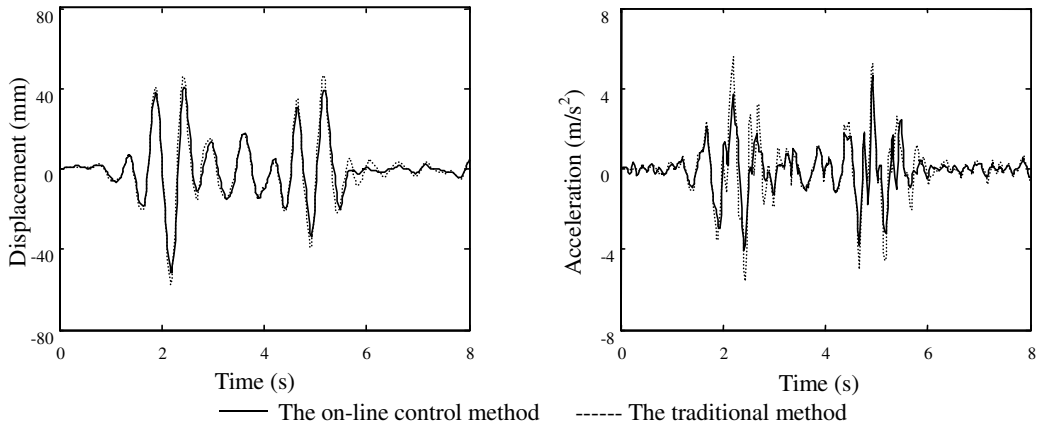

Figure 9. The responses comparison between the on-line control method and the traditional method.

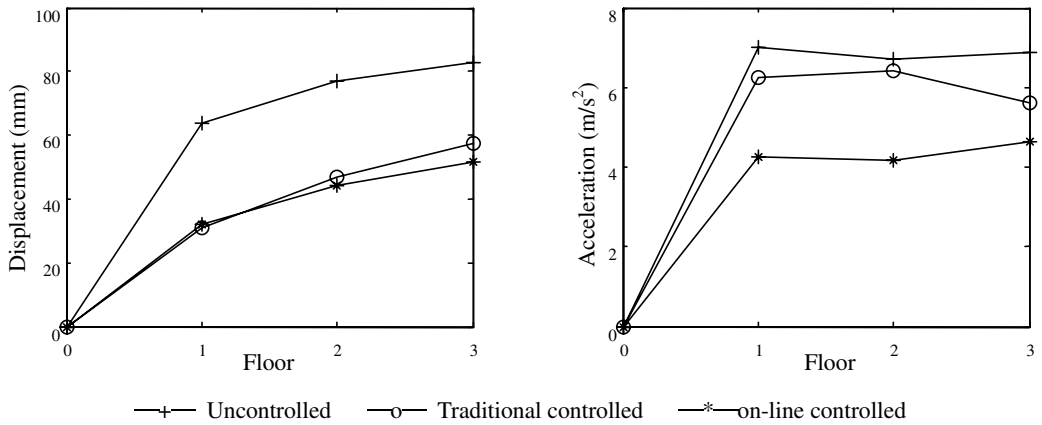

Figure 10. The maximum responses comparison of each floor.

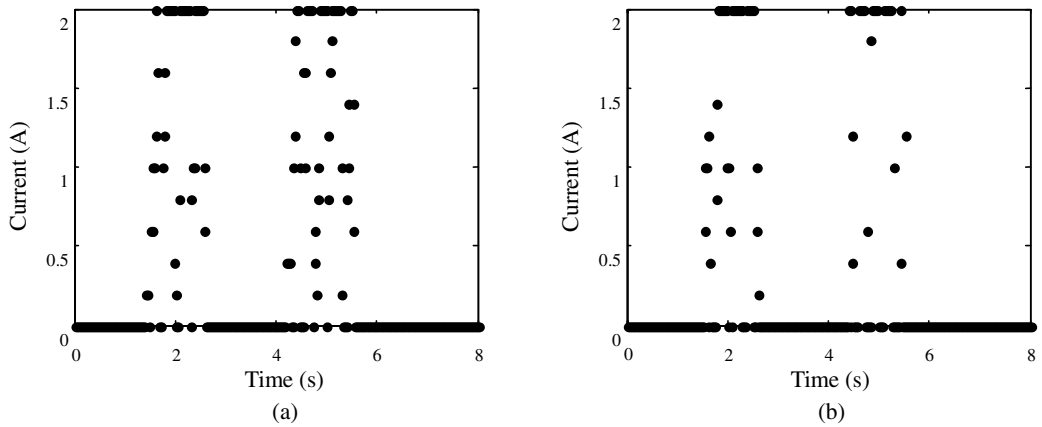

Figure 11. The relationship between the control current and time. (a) The on-line control method and (b) the traditional method.

period of 1.5–6.5 s. The control force produced by the MR damper changes in accordance with the responses of the structure, so that the responses of the structure are reduced more effectively.

It must be noted that the learning algorithm for the neural network is the LM algorithm and the objective error (MSE) is 5×10^{-5}. During the learning process, the LM algorithm has a very fast convergence rate. Only 0–10 training epochs are required to satisfy the objective error. Figure 12 shows the error convergence curve of training at the fifth earthquake sampling point. It can be shown that, when the training epochs reach 3, the error performance satisfies the objective error. Compared with the several thousand training epochs of the BP algorithm, the error convergence rate of the LM algorithm is very fast.

5. Conclusions

In this paper, a formula for MR dampers is derived according to the experimental data. Then an on-line real-time control method for semi-active control of earthquake-excited

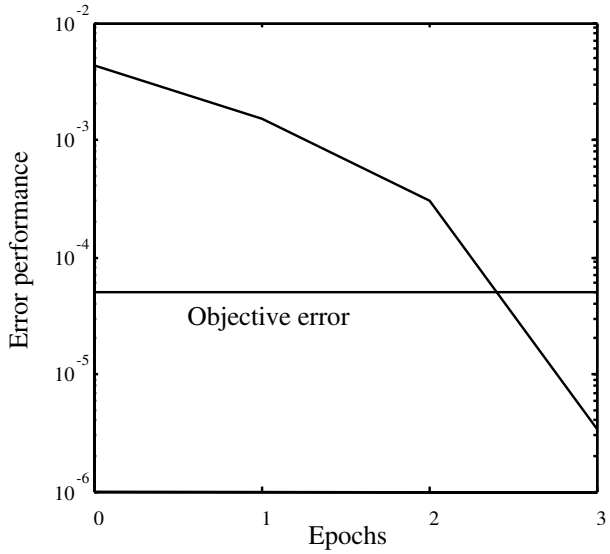

Figure 12. Training error convergence curve.

structures with MR dampers is proposed. In a numerical example, a three-storey smart structure with a MR damper in the first floor is analyzed. Some conclusions can be drawn from the analysis.

(1) The MR damper is a kind of smart damper, and it can reduce the responses of structures effectively.
(2) The yielding shear stresses calculated by equation (3) fit the experimental results very well.
(3) The on-line real-time control method solves the problem of time delay. The responses of the structure with MR dampers calculated by this method are smaller than those calculated by the traditional elastoplastic time-history method, especially for the acceleration responses.
(4) The LM algorithm is a second-order-convergence approach, which has a very fast convergence rate.

Acknowledgments

This research is financially supported by the National Natural Science Foundation, People's Republic of China, grant no 50135030, and the National Postdoctoral Science Foundation, People's Republic of China. These supports are gratefully acknowledged.

References

[1] Soong T T and Dargush G F 1997 *Passive Energy Dissipation Systems in Structural Engineering* (Chichester: Wiley)
[2] Soong T T, Masri S F and Housner G W 1991 An overview of active structural control under seismic loads *Earthq. Spectra* **7** 483–505
[3] Michael D S and Michael C C 1999 Semi-active control systems for seismic protection of structures: a state-of-the-art review *Eng. Struct.* **21** 469–87
[4] Kasparian V and Batur C 1998 Model reference based neural network adaptive controller *ISA Trans.* **37** 21–39
[5] Nikzad K, Ghaboussi J and Stanley L P 1996 Actuator dynamics and delay compensation using neurocontrollers *J. Eng. Mech., ASCE* **122** 966–75
[6] Liu G P and Daley S 1999 Output-model-based predictive control of unstable combustion systems using neural networks *Control Eng. Prac.* **7** 591–600
[7] Dyke S J, Spencer B F, Quast P and Sain M K 1995 Role of control-structure interaction in protective system design *J. Eng. Mech., ASCE* **121** 322–38
[8] Gallent S I 1993 *Neural Network Learning and Expert System* (Cambridge, MA: MIT Press)
[9] Chen H M, Tsai K H, Qi G Z, Yang J C S and Amini F 1995 Neural network for structural control *J. Comput. Civil Eng., ASCE* **9** 168–76
[10] Ghaboussi J and Joghataie A 1995 Active control of structures using neural networks *J. Eng. Mech., ASCE* **121** 555–67
[11] Yang S M and Lee G S 1997 Vibration control of smart structures by using neural networks *J. Dyn. Syst., Meas., Control, ASME* **119** 34–9
[12] Bani-Hani K, Ghaboussi J and Schneider S P 1999 Experimental study of identification and control of structures using neural network *Earthq. Eng. Struct. Dyn.* **28** 995–1018
[13] Ni Y Q, Chen Y, Ko J M and Cao D Q 2002 Neuro-control of cable vibration using semi-active magneto-rheological dampers *Eng. Struct.* **24** 295–307
[14] Xu Y L, Qu W L and Ko J M 2000 Seismic response control of frame structures using magnetorheological/ electrorheological dampers *Earthq. Eng. Struct. Dyn.* **29** 557–75
[15] Spencer B F, Dyke S J, Sain M K and Carlson J D 1997 Phenomenological model for magnetorheological dampers *J. Eng. Mech.* **123** 230–8
[16] Carlson J D and Spencer B F 1996 Magnetorheological fluid dampers: scalability and design issues for application to dynamic hazard mitigation *Proc. 2nd Int. Workshop on Structural Control (HongKong, 1996)* pp 99–109
[17] Dyke S J, Spencer B F, Sain M K and Carlson J D 1996 Modeling and control of magnetorheological dampers for seismic responses reduction *Smart Mater. Struct.* **5** 567–75
[18] Werely N M, Pang L and Kamath G M 1998 Idealized hysteresis modeling of electrorheological dampers *J. Intell. Mater. Syst. Struct.* **9** 642–9
[19] Xu Zhao-Dong and Shen Ya-Peng 2002 The calculating models and simulation analysis about magnetorheological damper *Build. Struct.* **9** 16–20 (in Chinese)
[20] Gavin G P, Hanson R D and Filisko F E 1996 Electrorheological dampers: part I. Analysis and design *J. Appl. Mech.* **63** 669–75
[21] Phillips R W 1969 Engineering applications of fluids with a variable yield stress *PhD Thesis* University of California, Berkeley
[22] Ou Jinpin and Guan Xinchun 1999 Experimental study of MR damper performance *Earthq. Eng. Eng. Vib.* **19** 76–81
[23] Clough R W and Penzien J 1975 *Dynamics of Structures* (New York: McGraw-Hill)
[24] Zeidenberg M 1990 *Neural Network Models in Artificial Intelligence* (New York: Horwood)
[25] Xu Z-D 2001 The experimental study on the (lead) viscoelastic structure *Doctor Thesis* Xi'an University of Architecture and Technology, China (in Chinese)
[26] Tan Y and Sain M 2000 Neural-networks-based nonlinear dynamic modeling for automotive engines *Neurocomputing* **30** 129–42
[27] Hagan M T and Menhaj M B 1994 Training feedforward networks with the Marquardt algorithm *IEEE Trans. Neural Netw.* **5** 989–93